How evolution draws trade-offs

Salomé Bourg [1], Laurent Jacob[1], Frédéric Menu[1], and Etienne Rajon[1]

[1]Univ Lyon, Université Lyon 1, CNRS, Laboratoire de Biométrie et Biologie Evolutive UMR5558, F-69622 Villeurbanne, France

Recent empirical evidence suggest that trade-off shapes can evolve, challenging the classica image of their high entrenchment. Here we model the evolution of the physiological mechanism that controls the allocation of resources to two traits, by mutating the expression and the conformation of its constitutive hormones and receptors. We show that trade-off shapes do indeed evolve in this model through the combined action of genetic drift and selection, such that their evolutionarily expected curvature and length depend on context. Despite this convergence at the phenotypic level, we show that a variety of physiological mechanisms may evolve in similar simulations, suggesting redundancy at the genetic level. We anticipate that more complex evolutionary scenarios should tighten this link between genotype and phenotype. This model should provide a useful framework to interpret the overly complex observations of both evolutionary endocrinology and evolutionary ecology.

I. Introduction

Evolutionary biologists have long known that heritable characters (or traits) usually do not vary independently from each others (Stearns, 1992; Roff, 1993). Such pleiotropy is thought to hinder adaptive evolution, both because it restricts the available combinations of traits and because mutations are less likely favorable when they impact many traits (Fisher, 1930; Orr, 2005; Paaby and Rockman, 2013; Hine et al., 2014). How pleiotropy evolves, and whether it is universal – *i.e.* every gene contribute, to some extent, to all traits – or restricted is the subject of an old but still ongoing debate (Wright, 1980; Wagner et al., 2008; Wagner and Zhang, 2011; Hill and Zhang, 2012; Wagner and Zhang, 2012).

For many traits – when scaled such that they correlate positively with fitness – pleiotropy takes the form of a negative relationship called trade-off (Cody, 1966; Gadgil and Bossert, 1970; Stearns, 1989). Although trade-offs are usually detected by fitting simple regression models (*e.g.* Charnov and Ernest, 2006; Walker et al., 2008; Mappes et al., 2004; Roff et al., 2002; Tucic et al., 2005; Roff et al., 2003; Andersson et al., 2002; Hanski et al., 2006), these relationships are not necessarily linear. Their precise shape is actually a major evolutionary parameter that, by constraining movements on fitness surfaces, conditions evolutionary outcomes (Levins, 1968; de Mazancourt and Dieckmann, 2004; Leslie et al., 2017; Verin et al., 2017; Pásztor et al., 2016). Trade-off shapes have long been considered inescapable constraints on the combination of traits that can exist, but this view is changing (Braendle et al., 2011; Garland Jr and Carter, 1994). Indeed, recent empirical work has shown that trade-off shapes are highly context-dependent, responding plastically to experimentally manipulated environmental changes (Jessup and Bohannan, 2008; Maharjan et al., 2013; Messina and Fry, 2003; Sgrò and Hoffmann, 2004). Moreover, trade-off shapes have been shown to change in a heritable manner, and evolve in organisms placed in experimentally manipulated environments (Roff et al., 2002; Leroi et al., 1994).

It is commonly accepted that negative relationships prevail because they result from the differential allocation of finite resources (Van Noordwijk and de Jong, 1986; Stearns, 1989; Agrawal et al., 2010; Stearns, 1992; Roff, 1993; Harshman and Zera, 2007; Reznick et al., 2000; Zera and Harshman, 2001). In multicellular organisms, resource allocation is regulated by hormones, whose joint effect on several traits creates so-called hormonal pleiotropy (Finch and Rose, 1995). For example, the internal concentration in juvenile hormone JH specifies the position – *i.e.* the combination of traits – along trade-offs between energetically-reliant traits like fecundity and survival in *Drosophila melanogaster* (Flatt, 2005) or fecundity and dispersal in *Gryllus firmus* (Zhao and Zera, 2002). Due to the key role of hormones as mediators of trade-offs, changes in the endocrine system are good candidates to explain the aforementioned plastic and heritable changes in trade-off shapes (Ketterson and Nolan Jr, 1992).

The question of how the endocrine system changes and responds to selection is addressed empirically by the emerging field of evolutionary endocrinology (Zera and Zhang, 1995; Cox et al., 2016*a*,*b*; Garland et al., 2016). This field, unfortunately, lacks a theoretical companion that would predict how endocrine systems should evolve depending, for instance, on the ecological context. The closest theory that has addressed related questions originated with van Noordwijk and de Jong's seminal paper (Van Noordwijk and de Jong, 1986), and was later improved by dynamic energy budget models (Kooijman, 1986, 2000; Jager et al., 2013). These models consider 'mutations' that modify resource allocation, thereby ignoring the regulatory and coding mutations impacting the proteins that actually form the endocrine system. Therefore, despite its momentous contribution to our understanding of

Corresponding author: *salome.bourg@univ-lyon1.fr*

evolution, this theory has presumably limited power to explain how the endocrine system and trade-off shapes should evolve.

Our aim with the present study is to initiate a theoretical reflection on how endocrine systems evolve. In this spirit, we built an evolutionary model where the interactions between hormones and receptors control the energy allocation to two trait-converting structures. This model considers mutations that can change the conformation and expression of hormones and receptors. We show that, through the appearance and fixation of these mutations, the shape of the trade-off between the two traits does indeed evolve. Furthermore, this shape is highly dependent on a rarely considered parameter, the cost associated with resource storage. Consequently, in the simple ecological setting considered here, evolutionarily expected trade-off shapes and their underlying endocrine mechanism should depend both on the resource that is traded, and on parameters that set the burden associated with storage structures

TRADE-OFF SHAPES DO EVOLVE

The conversion of an energetic resource into trait values is carried out by two specialized structures in our model, whose efficiency decreases as the inward flow of the resource increases (see SI figure 1). This flow is contingent on the dynamics of hormone-receptor binding at the surface of these structures, as newly formed hormone-receptor complexes activate inward transporters of the resource (see the *Material and methods* section for a precise, mathematical description of the model). Thus, following a meal – suddenly increasing the internal concentration of the resource – the resource may enter the converting structures, or a storage structure insofar as the internal concentration of the resource is above a threshold (figure 1). Past this threshold, the resource is instead released from the storage structure to maintain a constant internal concentration. Storage comes with a cost, such that the amount of the resource released may be lower than the amount that had actually been stored. After the storage structure has gone empty, the internal concentration of the resource decreases until it reaches a critically low value (figure 1). At this point, each individual's fitness is calculated as the sum of its trait values.

When gene expression noise is ignored, an individual's phenotype is entirely contingent on its genotype. Four independent genes code for two hormones and two receptors, whose expressions and conformations may change, respectively due to regulatory and coding mutations. These two types of mutation may impact the hormone-receptor dynamics, with potential effects on the resource allocation dynamics and thus on the trait values. These mutations change in frequency through the combined effect of drift and selection.

Our results show that trade-offs can, in principle, evolve. A representative example of the ongoing evolutionary dynamics is represented on figure 2-a. The population is initially monomorphic, so its occupies a single point on the phenotype space with low values

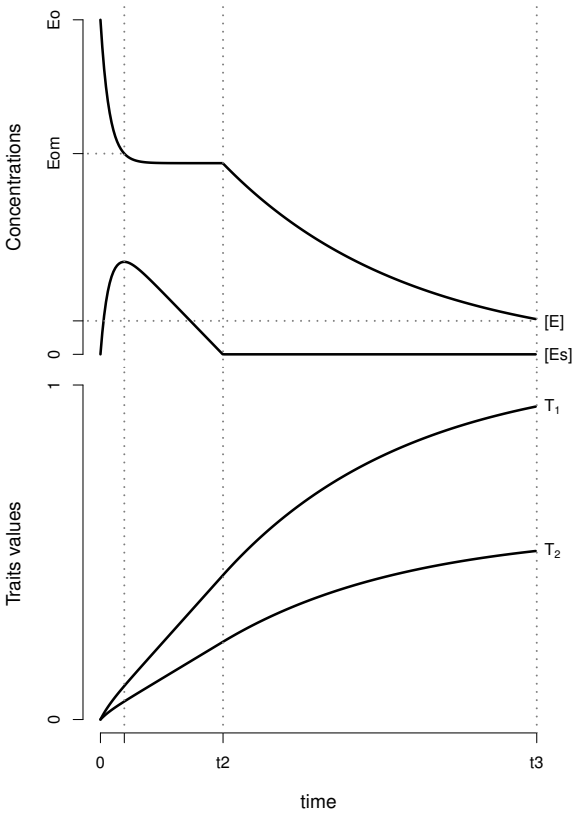

FIGURE 1: The final trait values, T_1 and T_2, depend on the dynamics of the concentration of the resource circulating the organism, $[E]$, and stored, $[E_s]$. $[E]$ starts at Eo immediately after a unique meal, and decreases as the resource is both stored ($[E_s]$ increases) and used by the two converting structures (T_1 and T_2 increase). As $[E]$ decreases below a threshold E_{om}, the resource is released from the storage structure ($[E_s]$ decreases), which compensates for the energy used and converted into traits T_1 and T_2. When no stored resource remains ($[E_s] = 0$), $[E]$ inevitably decreases (as T_1 and T_2 keep increasing), until it reaches a minimum threshold. The organism's final trait values T_1 and T_2 calculated at this point are used to assess its fitness. The hormones and receptors at the surface of the two converting structures control their resource intake, and thereby also the dynamics of $[E]$ and $[E_s]$, such that mutations of the expression and conformation of these proteins may change the organism's phenotype in a complex and unpredictable way. We used specific parameter values to obtain a clear illustration : $Eo = 1$, $E_{om} = 0.6$, $E_{min} = 0.1$, $a = 0.0001$, $C_{storage} = 0.1$, $\Omega = 0.1$, $b = 0.002$, $\omega = 0.1$

of traits 1 and 2. As genetic variation builds up in the population, the phenotypes spread along an almost linear relationship ($t = 1000$ in fig. 2-a). Around timestep 3800 trait 1 increases following a trajectory nearly parallel to the x-axis – in about half the simulations trait 2 instead increased. This change conveys a very sharp fitness increase because the population reaches a different isocline in the fitness landscape. Then the population roughly follows this isocline toward a point where trait 1 equals trait 2 ($t = 100000$ in fig. 2-a). This move in the phenotype space is actually associated with a slight increase in fitness, due to the higher

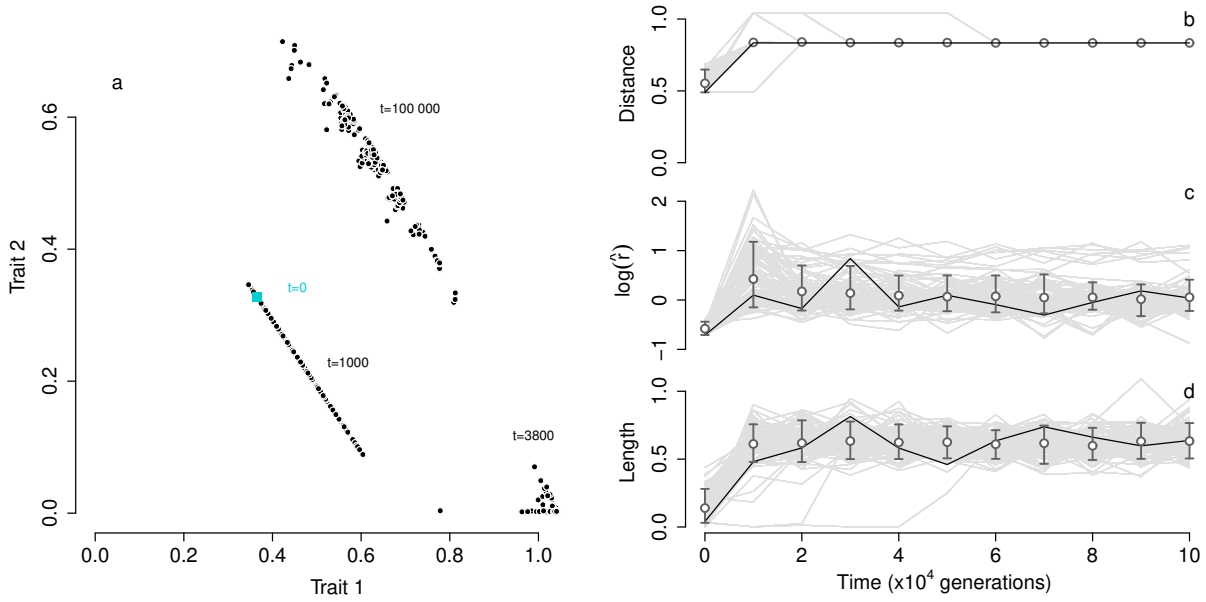

FIGURE 2: Trade-off shapes evolve in simulations where mutations change hormones' and receptors' conformation and expression, and selection acts depending on the resulting trait values. Panel a shows a few important timesteps in one representative simulation. We defined three parameters to study changes in shape systematically in an ensemble of 100 identically parameterized simulations, by fitting a circle to sets of points at regular timesteps (see text and *Material and methods section* II-E). Panel b shows the temporal dynamics of the distance of the median projection on the fitted circle to the origin. The natural logarithm of the fitted circle's radius (inversely related with the trade-off curvature) is represented in panel c, and the length of the trade-off (*i.e.* the distance along the circle between the two most distant projections) is represented in panel d. 99 replicate simulations are represented in grey in panels b-d, and the simulation in panel a is outlined in black. Dots and bar represent respectively the mean and quantiles (0.1 and 0.9) of each parameter's distribution (across simulations) at each timestep. Standard parameter values where used (as defined in the *Material and methods* section), and $C_{\text{storage}} = 0.7$.

efficiency of resource conversion when the two trait-converting structures are equally employed.

We identify changes in the shape of the trade-off by fitting a circle to the combinations of traits that coexisted at any time point in our simulations (see the *Material and methods* section II-E and figure 3). We projected each individual datapoint on the fitted circle, and calculated the Euclidean distance d of the median projection to the origin. Because d is closely related with fitness, it increases during the simulation (figure 2-b). The trade-off curvature decreases as the circle's radius $\hat{r}$ increases; we thus use $\log(\hat{r})$ as a negative proxy for curvature. As shown in figure 2-c, the curvature increases rapidly during the simulations. We also estimate the trade-off length as the distance between the two most distant projections on the circle, whose between-simulation mean quickly stabilizes to about 0.6 (figure 2-d).

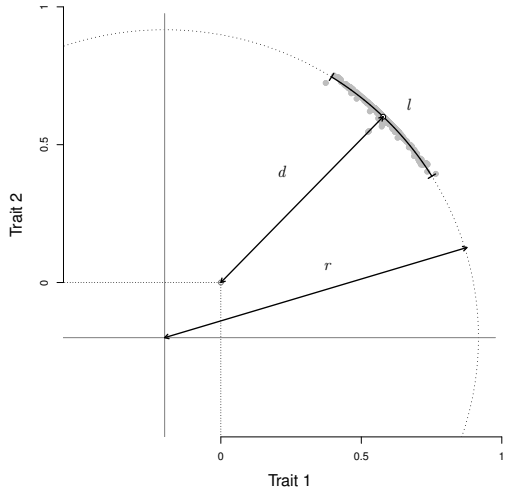

FIGURE 3: We extracted three descriptive parameters termed l (for length), d (for distance to the origin) and $\hat{r}$ (for radius) by fitting a circle to the phenotypes (trait 1, trait 2) at the end of our simulations. We minimized the squared distances of the orthogonal projection of individual datapoints to obtain $\hat{r}$ and the center of the circle (at the intersection of the horizontal and vertical lines). Then we calculated d as the distance of the median projection to the origin, and l as the distance along the circle between the two most distant projections.

THE EVOLUTION OF TRADE-OFF SHAPES DEPENDS ON STORAGE COST

As mentioned above, our model includes a parameter C_{storage} for the cost of storage, which in nature comes from two distinct sources. First, large molecules need to be produced for storage and later broken down at the time of release (Hers, 1976; Meyers, 1995; Alonso et al., 1995); second, maintaining storage structures can be costly and the added weight and volume might have negative consequences for the organism's fitness. The cost of producing storage molecules is

likely dependent on the resource : various types of molecules are ingested during a meal, with specific storage constraints (Williams et al., 1963). Carbohydrates like glucose, for instance, are stored under the form of glycogen, which is rapidly converted back into an energetic resource but requires a large amount of water – and thus a large volume and weight – for storage, contrary to lipids that are stored as fatty acids (Schmidt-Nielson, 1997). Specific advantages and disadvantages associated with each resource may translate into specific storage costs, likely in interaction with the ecology of the species considered. For example, the added weight might have a moderate fitness impact for marine species compared to aerial ones.

We varied this cost between 0 and 1 and found that the evolutionarily expected shape parameters drastically change in response (figure 4). As the cost increases, populations reach lower trait values (and are therefore at a lower distance to the origin, fig. 4-a), as an increasing part of their resources are inevitably wasted. Presumably, the genotypes that evolve under a specific storage cost optimize the speed of resource consumption. Faster consumption would lead to a less efficient energy conversion, while slower consumption would require storing more resources, and paying the associated cost. Under a high storage cost, selection thus favors rapid converters that allocate a similar amount of energy to each trait. A deviation from this ideal allocation decreases the efficiency of the most-used converting structure, which explain that the trade-off becomes more curved – *i.e.* that $\log(\hat{r})$ decreases – as the storage cost increases (fig. 4-b). The trade-off length, representative of the population's standing genetic variation, decreases conjointly (fig. 4), likely because extreme individuals on these highly curved trade-offs have low fitnesses.

A comparison of these results with those of a neutral model indicates that selection plays a major role in the evolution of trade-off shapes. Presumably due to the absence of selection for an optimum conversion speed, the curvature of trade-offs here evolves independently of the storage cost (fig. 4-b). The trade-off length, nonetheless, decreases slightly as the storage cost increases in the neutral model (fig. 4-c). This is likely linked to the parallel decrease in the distance from the origin d observed in figure fig. 4-a, since a low d limits the maximum length that trade-offs with any shape can reach.

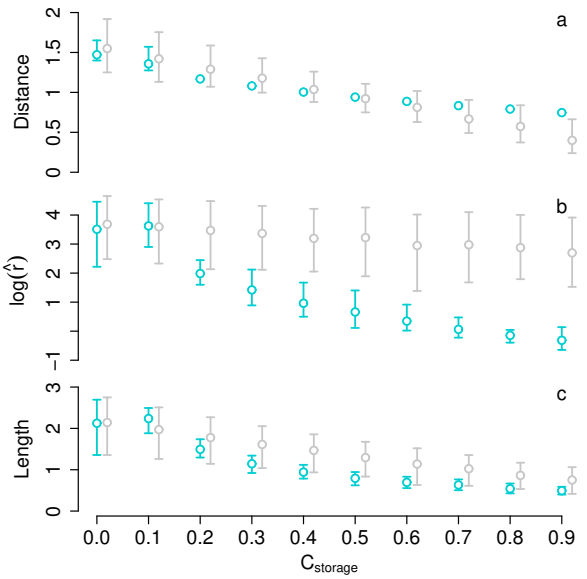

FIGURE 4: Evolutionarily expected shape parameters depend on the cost associated with storage C_{storage}, due to selection. The impact of selection appears by comparing the evolutionary expectations of a model with directional selection on both traits (in blue) with those of a neutral model (in grey ; individuals have identical fitnesses in this model, independent of their trait values). Definitions for the shape parameters can be found in the text, in the *Material and methods* section II-E, and in figs. 2,3.

How heritability evolves

Trade-off shape parameters such as the curvature remain rarely estimated in field or laboratory experiments. Heritability, however, is a common metric used in these studies to quantify the amount of variation along a trade-off on which selection may act. We quantified narrow sense heritability h^2 as the ratio of the additive genetic variance to the whole phenotypic variance in our simulations. Strikingly, this parameter is almost independent to the cost of storage (fig. 5-a) once this cost is above 0.1. The expected value of h^2 is then close to 0.5, which corresponds roughly to the most expected value in a compiled dataset of morphological traits (see figure 3 in ref. (Arnold, 2014).

While our predictions seem to match empirical observations on average, variance in observed values of h^2 is far greater than in our simulations, which is unlikely to be explained only by sampling noise. This illustrates that different traits may have different heritabilities, for instance due to particular ecological and population contexts. At this point, we are unable to consider using our model of arbitrary traits evolving in oversimplified ecological settings. Nonetheless, we can introduce a potentially important factor for the evolution of heritability that directly impacts the underlying physiological mechanisms : noise in gene expression. In figure 5-a as in the rest of the results presented so far, no noise was considered, such that the phenotype was entirely dependent on the genotype – h^2 is then lower than 1 due to dominance and epistasis. We modeled noise in gene expression by multiplying each gene expression by 10^{ϵ}, where ϵ is sampled from a normal distribution with mean 0 and standard deviation σ_{n}. As shown in figure 5-b, increasing σ_{n} decreases h^2 in a threshold-like manner : below $\epsilon = 0.5$, heritability remains close to its value in the absence of noise, while above this threshold h^2 rapidly vanishes – for comparison, mutations are modeled using a standard deviation $\sigma_{\text{m}} = 0.5$, such that if noise had the same effect as mutations h^2 would be close to 0.

We have also studied the impact of noise on the

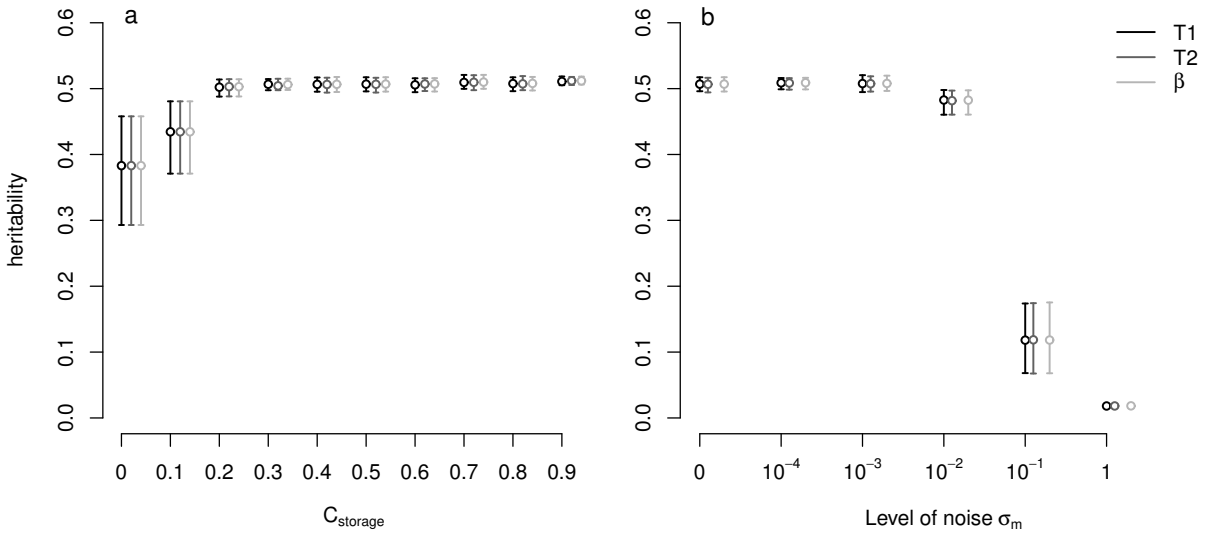

FIGURE 5: Evolutionarily expected heritabilities (narrow sense, h^2) are almost independent of the storage cost C_{storage} but are strongly impacted by increasing levels of noise (σ_n) in gene expression. h^2 was calculated as the ratio of the genetic additive variance to the phenotypic variance in populations evolved over 100000 generations, giving a distribution of values for each context (C_{storage},σ_m) considered. We represented the means (dots) and quantiles (0.1 and 0.9, bars) of these distributions. Performing calculations on trait 1 (T_1), trait 2 (T_2), or on the angle of each individual on the fitted circle (β, see *Material and methods* section II-E) has no visible impact on the results.

shape parameters of the trade-offs (SI figure 2). The curvature of the trade-off decreases as noise increases, which may have two distinct causes. First, more linear trade-offs may be selected as they make the organism robust to noise (Wagner, 2005; Draghi and Whitlock, 2015). Indeed, if the trade-off is more linear and aligns with the fitness isoclines, perturbations of gene expression levels still move individuals along trade-offs, but these moves have moderate fitness consequences. Second, noise has the effect of diminishing the strength of selection (Mineta et al., 2015). Hence, as noise increases in our simulations, it is possible that selection on the curvature weakens, such that the curvature decreases towards the neutral expectation (see figure 2).

THE LEVEL AT WHICH EVOLUTION CONVERGES

At this point we need to introduce the classical heuristic of genotype networks, which are made of nodes (each one a genotype) connected by mutations or recombination events (fig. 6 (Maynard Smith, 1970; Draghi et al., 2010; Rajon and Masel, 2013)). Typically, a genotype has a restricted number of neighbours relative to the total number of nodes in the network. When it harbors standing genetic variation (SGV), a population occupies a certain number of nodes on the network. Since SGV arises from short-lived mutations and recombination events (Barrett and Schluter, 2008; Lerouzic and Carlborg, 2008), the population likely occupies a small subset of the whole genotype space at any point in time. This subset defines the features of SGV, including a trade-off's shape. In the longer term, a population might make larger moves in the genotype space, changing its mutational neighborhood and thereby, possibly, the shape of its trade-off(s).

As we have seen, *e.g.* in figure 2, evolution is clearly convergent at the phenotype level – similar trade-off shapes evolve in similar contexts. We next ask whether evolution is also convergent at the physiological and genetic level. As anticipated by Garland and Carter (Garland Jr and Carter, 1994), convergence at these low levels would mean that organisms confronted to similar problems evolve identical mechanisms. This means that a unique neighborhood on the genotype space should yield a particular trade-off shape, as represented in figure 6-a.

We analyzed the genotypic variation in our evolved populations using a Principal Component Analysis (PCA) to test this hypothesis. Using the conformations of hormones and receptors in this analysis would be irrelevant, because the same affinity can be obtained by many pairs of hormone and receptor conformations. Instead, for each genotype, we identified the receptor that is closest in conformation to each hormone. Our first variable is the shortest difference in conformation, followed by the expression of the corresponding hormone and its population variance (we extracted the same variables for the second hormone). We also included in our dataset the concentrations of receptors and the ratios of these concentrations on the two converting structures. Under the assumption that only a single neighborhood can produce a specific trade-off shape, this analysis should reveal an association between the context (here the storage cost) and the genotype. Contrary to our expectation, however, this analysis revealed no structure in the genotypic data associated with the storage cost (fig. 7).

Therefore, evolution is not convergent at the genotype level – the evolutionarily expected genotype cannot be predicted from context. This may be explained by redundancy at the genotype level, such that

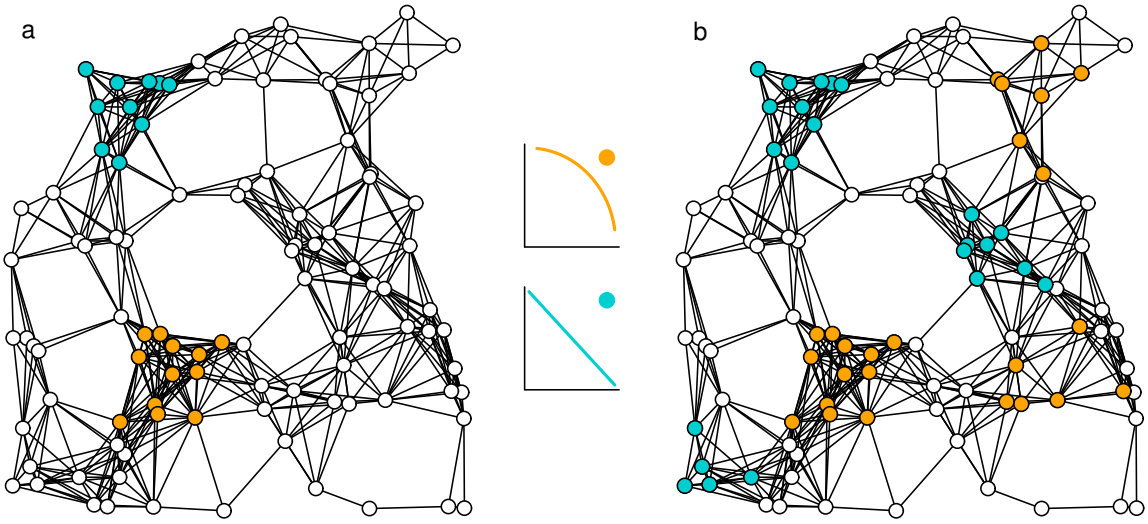

FIGURE 6: Two genotype spaces illustrate the two hypothesized relationships between the genotype (and hence the physiological mechanism) and the phenotype. Genotypes are represented by nodes, linked by mutations or recombination events. The phenotype is specified by a color for some genotypes, corresponding to the trade-off shapes represented in the center of the figure. In panel a, the two colored mutational neighborhoods are unique solutions to generate a given trade-off shape (no redundancy), whereas in panel b several mutational neighborhoods can lead to similar phenotypes (redundancy at the genotype level).

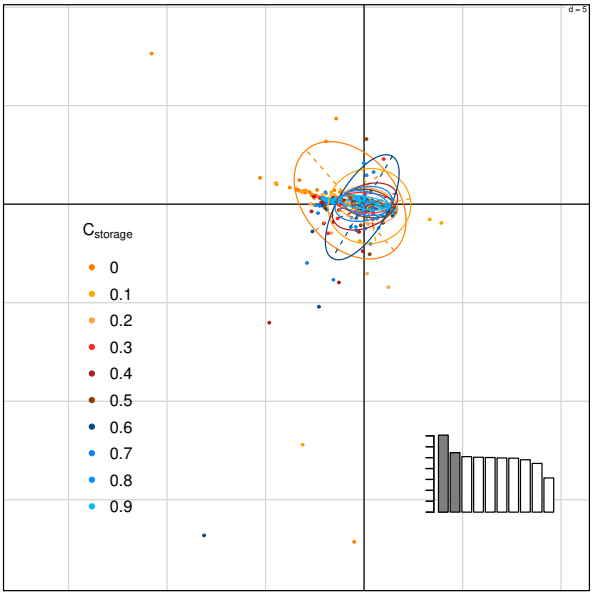

FIGURE 7: A PCA on genetically encoded physiological variables at the end of our simulations shows no association between these variables and the context, here represented by the storage cost (C_{storage}). The two first axes of the PCA are shown, whose relative contribution to the overall variance is shown in grey on the barplot in the bottom right part of the main panel.

several subsets of the genotype space produce similar phenotypes, as illustrated in figure 6-b. At first sight, this prediction seems incompatible with empirical observations indicating that major regulators in endocrine mechanisms are strongly conserved (Tatar et al., 2003; Barbieri et al., 2003), suggesting that evolution has found few solutions to a given problem. However, this observation could also be explained by a specific structure of the genotype space preventing large evolutionary moves between similar neighborhoods. This situation can be pictured in the hypothetical genotype space in figure 6-b by giving genotypes represented by white dots very low fitnesses : changes in trade-off shapes are still possible (some 'orange' genotypes have 'blue' neighbors) but reaching distant neighborhoods is highly unlikely.

Importantly, this apparent discrepancy between observations and predictions might be due to a necessary lack of details in our model. Our model is a first step toward an evolutionary theory inclusive of physiological mechanisms and phenotypic relationships. We thus leave the role of examining which details are important to future studies. We foresee that more complex physiological mechanisms that, for instance, respond to environmental and physiological cues, might be achieved by more restricted sets of genotypes. This could create a closer association between genotype and phenotype, and explain that regulatory mechanisms are so conserved in nature.

Nonetheless, despite its simplicity the model presented here does produce physiological features that are also observed in nature. For example, we have found that the affinity between hormone and receptor is generally lower than its maximum possible value (SI figure 2), similar to observations in rats (Blair et al., 2000). While this lower-than-maximum affinity is sometimes associated with faster responses to changes in hormone concentrations, such reactivity does not provide a selective advantage in our model. Instead a lower-than-maximum affinity could evolve because it optimizes the rate of hormone-receptor binding at

equilibrium. Indeed, selection favors an increase in the speed of resource consumption as the cost of storing resources increases – because consuming slowly, and thus storing resources, is costly – which is limited by the inefficiency of converting resources into traits as the speed increases. In figure SI figure 2, we see that faster consumption is at least partly achieved in our model by increasing the affinity between hormones and receptors, but that the distance in conformation remains positive even for very high costs of storage.

II. Materials and methods

The model considers the conversion of an energetic resource by specialized structures into two traits under directional selection. Hormones may bind a surface's receptor, which activates inward transporters of the resource. We assume that the resource intake ("meal" thereafter) takes place once the hormone-receptor dynamics has reached its unique equilibrium (studied in subsection II-A). The model then considers the dynamical absorption of the resource by the two converting structures as well as exchanges with a storage structure (subsection II-B). The energy accumulated by structures is immediately converted into two traits values (subsection II-C). We let this physiological mechanism change by mutation and evolve under the influence of selection and drift as described in subsection II-D, and analyse these simulation results as described in subsection II-E.

A. Hormone-receptor binding dynamics

A single structure produces two hormones whose internal concentrations are denoted $[H_k]$ (with $k \in \{1,2\}$), and another structure degrades them. Two structures converting energy into traits express receptors on their surface. The concentration of receptors of type i on structure j is denoted $[R_{ij}]$ (we ignore the specific processes of production and degradation of receptors). Hormone k and receptor i form complexes at rate $k_{\text{on}_{ik}}$ (depending on their respective conformations, see *Hormone-receptor binding affinity*), and complexes dissociate at rate k_{off} . The concentration of complexes formed between receptor i and hormone k on structure j is denoted $[R_{ij}H_k]$. The hormone-receptor binding dynamics are described by the generic equations [1]-[5] below. n_{r} and n_{s} are respectively the number of receptor types and the number of converting structures.

Free circulating hormones. The concentration of hormone k, $[H_k]$, increases as the hormone is produced at a rate α_k (first term in equation [1]) and as hormone-receptor complexes dissociate at a rate k_{off}. All n_{r} receptors on each structure are considered in the second term of equation [1]. $[H_k]$ decrease as complexes form (third term) at rate $k_{\text{on}_{ik}}$ specific of the receptor type i and of the hormone k, and due to unspecific hormone degradation (last term).

$$\frac{d[H_k]}{dt} = \alpha_k + \sum_{i=1}^{n_{\text{r}}}\sum_{j=1}^{n_{\text{s}}}\Big((k_{\text{off}} \times [R_{ij}H_k]) - (k_{\text{on}_{ik}} \times [R_{ij}] \times [H_k])\Big) - k_d \times [S_{\text{D}}] \times [H_k] \quad (1)$$

Free receptors. The number of free receptors increases as complexes dissociate and decreases as complexes form with each of the n_{h} hormones produced by the organism (equation [2]).

$$\frac{d[R_{ij}]}{dt} = \sum_{k=1}^{n_{\text{h}}}((k_{\text{off}} \times [R_{ij}H_k]) - (k_{\text{on}_{ik}} \times [R_{ij}] \times [H_k])) \quad (2)$$

Hormone-receptor complexes. The number of hormone-receptor complexes increases as hormones bind on receptors and decreases as complexes dissociate (equation [3])

$$\frac{d[R_{ij}H_k]}{dt} = k_{\text{on}_{ik}} \times [R_{ij}] \times [H_k] - k_{\text{off}} \times [R_{ij}H_k] \quad (3)$$

The concentration of receptor i is constant ($[R_{ij\text{tot}}] = [R_{ij}] + \sum_{k=1}^{n_{\text{h}}}[R_{ij}H_k]$), such that each dissociated complex releases a free receptor and each formed complex monopolizes a free receptor.

Degradation structure. Our model includes a structure which degrades hormones non specifically through endocytosis. The liver can be considered an example of such structure, which degrades the growth hormone (Baumann et al., 1987), insulin (Duckworth et al., 1998) and glucagon (Deacon, 2005). The dynamics of the concentration of free degradation sites $[S_{\text{D}}]$ and of degradation sites occupied by hormone k, $[S_{\text{D}}H_k]$ are described by equations [4] and [5]. The first term in each of these equations relies on the assumption that degradation sites are instantly freed.

$$\frac{d[S_{\text{D}}]}{dt} = \sum_{k=1}^{n_{\text{h}}}(([S_{\text{D}}H_k]) - (k_d \times [S_{\text{D}}] \times [H_k])) \quad (4)$$

$$\frac{d[S_{\text{D}}H_k]}{dt} = -[S_{\text{D}}H_k] + (k_d \times [S_{\text{D}}] \times [H_k]). \quad (5)$$

We set the total number of degradation sites $[S_{\text{D}}] + \sum_{k=1}^{2}[S_{\text{D}}H_k]$ to 9.9×10^{-4}, and the rate of hormone internalization k_{d} to 4.10^{-5} (Pearce et al., 1999) ; we did not allow these parameters to change by mutation. Other parameters in the model, however, can mutate and change the equilibrium concentration of the free hormone (*e.g.* the rate of production of each hormone). As described in the section *Evolutionary and population dynamics*, we randomly drew the values of mutable parameters at the beginning of each simulation from known distributions, and verified that the internal hormonal concentration at equilibrium is, initially, within the range $5.10^{-12} - 10^{-8}$ M, in accordance with

experimental data (Polonsky et al., 1988; Zadik et al., 1985).

Hormone-receptor binding equilibrium. Hormone-receptor binding dynamics eventually reach an equilibrium where $[H_k]$, $[R_{ij}]$ and $[R_{ij}H_k]$ are stable (equilibrium values are identifed by a star in equations [6]-[8], obtained by solving the system formed by equations [1]-[5] (see details in supplement).

$$[H_k]^* = \frac{\alpha_k}{k_{\text{d}} \times [RD]^*} \tag{6}$$

$$[R_{ij}]^* = \frac{[R_{ij\text{tot}}]}{\sum_{k=1}^{n_h} (\frac{[H_k]^* \times k_{\text{on}_{ik}}}{k_{\text{off}}}) + 1} \tag{7}$$

$$[R_{ij}H_k]^* = \frac{[R_{ij}]^* \times [H_k]^* \times k_{\text{on}_{ik}}}{k_{\text{off}}} \tag{8}$$

B. Energy allocation dynamics

An individual takes a unique meal at t_0 which sets its internal concentration of an energetic resource $[E]$ to $Eo = 1$. Then $[E]$ decreases, as the resource is partly stored and partly allocated to two structures converting it into traits values. Despite some simplifying assumptions detailed below, we consider that receptors in our model function like G protein coupled receptors, whose activation produces an internal signal for a limited amount of time, followed by their internalization and recycling into free receptors. In our model, newly formed hormone-receptor complexes instantaneously stimulate transporters of the resource and become inactive. The number of complexes formed on structure j per time unit at equilibrium equals :

$$a_j = \sum_{k=1}^{n_h} \sum_{i=1}^{n_r} (k_{\text{on}_{ik}} \times [R_{ij}]^* \times [H_k]^*) \tag{9}$$

which we multiplied by a constant $C_f = 1000$ to obtain the inward flow of energy for this structure.

Hormone-receptor complexes normally dissociate at a rate k_{off} of the order of $10^{-4} - 10^{-5}$ (Pearce et al., 1999). We voluntarily over-estimated this rate ($k_{\text{off}} = 0.1$) to model recycling, thereby considering that both the hormone and the receptor are released when recycling is completed. With this parameterization, a receptor is recycled within 10 minutes on average, which is biologically realistic (von Zastrow 1992).

Considering that both the hormone and the receptor are released is mathematically convenient but unrealistic, as recycling is most often followed by the degradation of the hormone. We verified using numerical simulations, where the hormone is indeed not released, that this assumption does not impact our results (see SI figure 3). The energy allocation dynamics consider temporal changes in $[E]$ as well as in $[E_s]$, the concentration of the resource stored. The ODE for the instant changes in $[E]$ and $[E_s]$ are given below (equations [10]-[11]) :

$$\frac{dE}{dt} = \begin{cases} -a \times E - b \times (E - E_{\text{om}}), & \text{if } E > E_{\text{om}} \\ -a \times E & \text{otherwise} \end{cases} \tag{10}$$

$$\frac{dEs}{dt} = \begin{cases} b \times (E - E_{\text{om}}) \times (1 - C_{\text{storage}}), & \text{if } E > E_{\text{om}} \\ b \times (E - E_{\text{om}}), & \text{if } E < E_{\text{om}} \text{ and } Es > 0 \\ 0 \text{ otherwise,} \end{cases} \tag{11}$$

with $a = \sum_{j=1}^{n_s} a_j \times C_{\text{f}}$ and $b = 0.01$.

We solved these equations (see SI text 1) and obtained the temporal dynamics, $[E](t)$ and $[E_s](t)$ by separating them into three phases illustrated in figure 1. Phase 1 starts at t_0 (the meal) and goes on as long as $[E] > E_{\text{om}}$, $E_{\text{om}} = 0.08$ being a concentration threshold above which energy is stored. During phase 2 – which starts at t_1 (when $[E] = E_{\text{om}}$) – the resource is released from the storage structure which compensates for its consumption by converting structures. Phase 3 begins when $[E_s]$ reaches 0, such that $[E]$ decreases until it reaches the critically low value $E_{\text{min}} = 0.01$.

C. Energy conversion into traits

The energy allocated to each structure is converted into an increase of trait value 1 (for structure 1) and trait value 2 (for structure 2). Traits are deliberately abstract, but their biological relevance is quite obvious. For example, energy allocation to reproductive structures can increase the quality and number of gametes, thus increasing fertility. Likewise, energy allocation to somatic maintenance or camouflage may increase survival. Here we assume that allocating a lot of energy to one structure per time unit decreases the efficiency of conversion. The observation that fast feeding larvae of *D. melanogaster* have lower fitness than slow feeding larvae may support this assumption (Foley and Luckinbill, 2001; Prasad and Joshi, 2003; Mueller et al., 2005; Roff and Fairbain, 2007), although it could also be partly explained by increased efficiency of digestion in slow feeding larvae. It is obvious, however, that some loss will occur as energy expenditure increases, as no organism is capable of instantly using large amounts of resources. We model this loss as :

$$\frac{dT_j}{dt} = \frac{\omega \times a_j \times [E] \times C_{\text{f}}}{\Omega + a_j \times [E] \times C_{\text{f}}} \tag{12}$$

T_j is the trait value for structure j, $\omega = 0.02$ is the maximum increase of trait value per dt, and $\Omega = 0.01$ sets the speed with which this function saturates. We found the analytical expression of $T_j(t)$, which follows the dynamics of $[E](t)$ described above (see figure 1). The combination of trait values calculated at time t_3 is the phenotype of the individual, used to calculate its fitness (see below).

D. Evolutionary and population dynamics

The population is formed of $\frac{N}{2}$ females and $\frac{N}{2}$ males. Offspring production is modeled using a

Wright-Fisher process (Fisher, 1930; Wright, 1931), meaning that the population is entirely renewed at each timestep and that each newborn's two parents are sampled with probability p_i from the female and male pools. The genotype comprises four independent genes encoding two receptors and two hormones. An allele at the gene coding for receptor i determines its expression on each structure j, $[R_{ij\text{tot}}]$, and its conformation ΨR_i. Similarly, an allele at the gene coding for hormone k sets its production rate α_k and its conformation ΨH_k.

Individuals are diploid, and upon reproduction gametes are formed by sampling independently alleles for each gene from the two parental chromosomes. In the neutral instance of our model, the probability that mother or father i is drawn equals $p_i = \frac{N}{2}$. In the model with selection, the probability p_i that parent i is drawn is proportional to its fitness W_i :

$$p_i = \frac{W_i}{\sum_{j=1}^{\frac{N}{2}} W_j} \tag{13}$$

where $W_i = T_{1i} + T_{2i}$.

Therefore, this model includes genetic drift (a genotype can go extinct by chance) and selection.

Mutations. An allele's contribution to the protein's expression or conformation can mutate with probability $\mu = 10^{-4}$ per regulatory/coding sequence per generation. Mutations can change a receptor's concentration $[R_{ij\text{tot}}]$ or an hormone's production α_k. In this case, the mutant's value is multiplied by 10^{γ}, where γ is sampled from a normal distribution with mean 0 and standard deviation $\sigma_m = 0.5$. Conformations are modeled as a number in the set of positive integers $\{1; 1000\}$. Coding mutations can change this number by adding an integer sampled from a discretized normal distribution with mean 0 and standard deviation 1, and from which 0 values were excluded to avoid neutral mutations.

The specific on-rate constant, $k_{\text{on}_{ik}}$, for hormone k and receptor i depends on their respective conformations according to equation [14].

$$k_{\text{on}_{ik}} = \kappa \times e^{(-\rho \times |\Psi H_k - \Psi R_i|)} \tag{14}$$

Affinity between hormone k and receptor i is maximum when $\Psi H_k = \Psi R_i$, and decreases as the difference between these numbers increases. Affinity may thus change as the receptor's or the hormone's conformation mutates.

Initial conditions. Each population at $t = 0$ is monomorphic, such that all individuals share the same genotype and are homozygotes for all genes. We nonetheless introduced variation in the initial genotypes across replicate simulations, by mutating every coding and regulatory sequence once from an average starting genotype. This average genotype produces hormones at rate $\alpha_k = 9.9 \times 10^{-10}$ ($k \in \{1, 2\}$) and expresses $[R_{ij\text{tot}}] = 9.9 \times 10^{-5}$ receptors of type i at the surface of structure j ($i \in \{1, 2\}$, $j \in \{1, 2\}$), and has hormones and receptors conformations $\Psi H_1 = 9$, $\Psi H_2 = 109$, $\Psi R_1 = 29$, and $\Psi R_2 = 129$.

E. Estimates of shape parameters

As described in the previous section, the physiological mechanism can change by mutations and evolve. We expect at least some of these mutation to have consequences on the shape of the trade-off between traits 1 and 2. We estimated these changes by fitting a circle to individual coordinates in the phenotype space formed by these traits. Because no causal relationship should be expected between trait 1 and trait 2, we performed an orthogonal regression to obtain estimates of the radius of the most fit circle $\hat{r}$ and the coordinates of its center (x_c, y_c) (Coope, 1993). From these estimates, we calculated three important parameters that quantify the curvature, the length and the position of the trade-off.

The curvature increases as the radius or its logarithm, $\log(\hat{r})$, decreases – obtaining $\log(\hat{r})$ is straightforward from the analysis. The length l – which is representative of the standing genetic variation in the population – is the distance between the two most distant orthogonal projections on the fitted circle. To obtain it, we first calculated the angle of each individual i as $\beta_i = \text{sign}(T_{2i} - y_c) \times \cos^{-1}(\frac{T_{1i} - x_c}{r_i})$, with r_i the Euclidean distance between (T_{1i}, T_{2i}) and (x_c, y_c) using a gradient descent method. Then we calculated $l = \hat{r} \times (\max(\beta) - \min(\beta))$. The position is evaluated by the distance of the median projection to the origin, d – a proxy for fitness, which we use in the neutral and in the selection model alike. We extracted the median angle in the distribution of β_i, β_M, and calculated the distance to the origin $d = \sqrt{(x_c + \cos(\beta_M) \times \hat{r})^2 + (y_c + \sin(\beta_M) \times \hat{r})^2}$.

RÉFÉRENCES

Agrawal, A. A., J. K. Conner, and S. Rasmann. 2010. Tradeoffs and negative correlations in evolutionary ecology. Evolution since Darwin : the first 150 :243–268.

Alonso, M., J. Lomako, W. Lomako, and W. Whelan. 1995. A new look at the biogenesis of glycogen. The FASEB journal 9 :1126–1137.

Andersson, S., S. R. Pryke, J. Örnborg, M. J. Lawes, and M. Andersson. 2002. Multiple receivers, multiple ornaments, and a trade-off between agonistic and epigamic signaling in a widowbird. The American Naturalist 160 :683–691.

Arnold, S. J. 2014. Phenotypic evolution : The ongoing synthesis. Am Nat 183.

Barbieri, M., M. Bonafè, C. Franceschi, and G. Paolisso. 2003. Insulin/igf-i-signaling pathway : an evolutionarily conserved mechanism of longevity from yeast to humans. American Journal of Physiology-Endocrinology And Metabolism 285 :E1064–E1071.

Barrett, R., and D. Schluter. 2008. Adaptation from standing genetic variation. Trends in Ecology & Evolution 23 :38–44.

Baumann, G., K. D. D. Amburn, and T. A. Buchanan. 1987. The effect of circulating growth hormone-binding protein on metabolic clearance, distribution, and degradation of human growth hormone. The Journal of Clinical Endocrinology & Metabolism 64 :657–660.

Blair, R. M., H. Fang, W. S. Branham, B. S. Hass, S. L. Dial, C. L. Moland, W. Tong, L. Shi, R. Perkins, and D. M. Sheehan. 2000. The estrogen receptor relative binding affinities of 188 natural and xenochemicals : structural diversity of ligands. Toxicological Sciences 54 :138–153.

Braendle, C., A. Heyland, and T. Flatt. 2011. Integrating mechanistic and evolutionary analysis of life history variation. Mechanisms of life history evolution : the genetics and physiology of life history traits and trade-offs pages 3–10.

Charnov, E. L., and S. M. Ernest. 2006. The offspring-size/clutch-size trade-off in mammals. The American Naturalist 167 :578–582.

Cody, M. L. 1966. A general theory of clutch size. Evolution pages 174–184.

Coope, I. D. 1993. Circle fitting by linear and nonlinear least squares. Journal of Optimization Theory and Applications 76 :381–388.

Cox, R. M., J. W. McGlothlin, and F. Bonier. 2016*a*. Evolutionary endocrinology : Hormones as mediators of evolutionary phenomena : An introduction to the symposium. Integrative and Comparative Biology 56 :121–125.

———. 2016*b*. Hormones as mediators of phenotypic and genetic integration : an evolutionary genetics approach. Integrative and Comparative Biology 56 :126–137.

de Mazancourt, C., and U. Dieckmann. 2004. Trade-off geometries and frequency-dependent selection. The American Naturalist 164 :765–778.

Deacon, C. F. 2005. What do we know about the secretion and degradation of incretin hormones ? Regulatory peptides 128 :117–124.

Draghi, J., and M. Whitlock. 2015. Robustness to noise in gene expression evolves despite epistatic constraints in a model of gene networks. Evolution 69 :2345–2358.

Draghi, J. A., T. L. Parsons, G. P. Wagner, and J. B. Plotkin. 2010. Mutational robustness can facilitate adaptation. Nature 463 :353.

Duckworth, W. C., R. G. Bennett, and F. G. Hamel. 1998. Insulin degradation : progress and potential. Endocrine reviews 19 :608–624.

Finch, C. E., and M. R. Rose. 1995. Hormones and the physiological architecture of life history evolution. The Quarterly Review of Biology 70 :1–52.

Fisher, R. A. 1930. The genetical theory of natural selection : a complete variorum edition. Oxford University Press.

Flatt, T. 2005. The evolutionary genetics of canalization. The Quarterly review of biology 80 :287–316.

Foley, P. A., and L. Luckinbill. 2001. The effects of selection for larval behavior on adult life-history features in drosophila melanogaster. Evolution 55 :2493–2502.

Gadgil, M., and W. H. Bossert. 1970. Life historical consequences of natural selection. The American Naturalist 104 :1–24.

Garland, T., M. Zhao, and W. Saltzman. 2016. Hormones and the evolution of complex traits : Insights from artificial selection on behavior. Integrative and Comparative Biology 56 :207–224.

Garland Jr, T., and P. Carter. 1994. Evolutionary physiology. Annual Review of Physiology 56 :579–621.

Hanski, I., M. Saastamoinen, and O. Ovaskainen. 2006. Dispersal-related life-history trade-offs in a butterfly metapopulation. Journal of Animal Ecology 75 :91–100.

Harshman, L. G., and A. J. Zera. 2007. The cost of reproduction : the devil in the details. Trends in Ecology & Evolution 22 :80–86.

Hers, H. 1976. The control of glycogen metabolism in the liver. Annual review of biochemistry 45 :167–190.

Hill, W. G., and X.-S. Zhang. 2012. Assessing pleiotropy and its evolutionary consequences : pleiotropy is not necessarily limited, nor need it hinder the evolution of complexity. Nature reviews. Genetics 13 :296.

Hine, E., K. McGuigan, and M. W. Blows. 2014. Evolutionary constraints in high-dimensional trait sets. The American Naturalist 184 :119–131.

Jager, T., B. T. Martin, and E. I. Zimmer. 2013. Debkiss or the quest for the simplest generic model of animal life history. Journal of theoretical biology 328 :9–18.

Jessup, C. M., and B. J. M. Bohannan. 2008. The shape of an ecological trade-off varies with environment. Ecology Letters 11 :947–959.

Ketterson, E. D., and V. Nolan Jr. 1992. Hormones and life histories : an integrative approach. The American Naturalist 140 :S33–S62.

Kooijman, S. 1986. Energy budgets can explain body size relations. Journal of Theoretical Biology 121 :269–282.

Kooijman, S. A. L. M. 2000. Dynamic energy and mass budgets in biological systems. Cambridge university press.

Leroi, A. M., S. B. Kim, and M. R. Rose. 1994. The evolution of phenotypic life-history trade-offs : an experimental study using drosophila melanogaster. The American Naturalist 144 :661–676.

Lerouzic, A., and O. Carlborg. 2008. Evolutionary potential of hidden genetic variation. Trends in Ecology & Evolution 23 :33–37.

Leslie, M. P., D. E. Shelton, and R. E. Michod. 2017. Generation-time and fitness trade-offs during the evolution of multicellularity. Journal of Theoretical Biology .

Levins, R. 1968. Evolution in changing environments : some theoretical explorations. 2. Princeton University Press.

Maharjan, R., S. Nilsson, J. Sung, K. Haynes, R. E.

Beardmore, L. D. Hurst, T. Ferenci, and I. Gudelj. 2013. The form of a trade-off determines the response to competition. Ecology Letters 16 :1267–1276.

Mappes, T., E. Koskela, and C. Lopez-Fanjul. 2004. Genetic basis of the trade-off between offspring number and quality in the bank vole. Evolution 58 :645–650.

Maynard Smith, J. 1970. Natural selection and the concept of a protein space. Nature 225 :563–564.

Messina, F. J., and J. Fry. 2003. Environment-dependent reversal of a life history trade-off in the seed beetle callosobruchus maculatus. Journal of evolutionary biology 16 :501–509.

Meyers, R. A. 1995. Molecular biology and biotechnology : a comprehensive desk reference. John Wiley & Sons.

Mineta, K., T. Matsumoto, N. Osada, and H. Araki. 2015. Population genetics of non-genetic traits : Evolutionary roles of stochasticity in gene expression. Gene 562 :16–21.

Mueller, L. D., D. G. Folk, N. Nguyen, P. Nguyen, P. Lam, M. R. Rose, and T. Bradley. 2005. Evolution of larval foraging behaviour in drosophila and its effects on growth and metabolic rates. Physiological Entomology 30 :262–269.

Orr, H. A. 2005. The genetic theory of adaptation : a brief history. Nature Reviews Genetics 6 :119–127.

Paaby, A. B., and M. V. Rockman. 2013. The many faces of pleiotropy. Trends in Genetics 29 :66–73.

Pásztor, L., Z. Botta-Dukát, G. Magyar, T. Czárán, and G. Meszéna. 2016. Theory-based ecology : A Darwinian approach. Oxford University Press.

Pearce, K. H., B. C. Cunningham, G. Fuh, T. Teeri, and J. A. Wells. 1999. Growth hormone binding affinity for its receptor surpasses the requirements for cellular activity. Biochemistry 38 :81–89.

Polonsky, K., B. Given, L. Hirsch, E. Shapiro, H. Tillil, C. Beebe, J. Galloway, B. Frank, T. Karrison, and E. Van Cauter. 1988. Quantitative study of insulin secretion and clearance in normal and obese subjects. Journal of Clinical Investigation 81 :435.

Prasad, N., and A. Joshi. 2003. What have two decades of laboratory life-history evolution studies ondrosophila melanogaster taught us ? Journal of genetics 82 :45–76.

Rajon, E., and J. Masel. 2013. Compensatory evolution and the origins of innovations. Genetics 193 :1209–1220.

Reznick, Nunney, and Tessier. 2000. Big houses, big cars, superfleas and the costs of reproduction. Trends Ecol Evol 15 :421–425.

Roff, D. 1993. Evolution of life histories : theory and analysis. Springer Science & Business Media.

Roff, D., P. Crnokrak, and D. Fairbairn. 2003. The evolution of trade-offs : geographic variation in call duration and flight ability in the sand cricket, gryllus firmus. Journal of evolutionary biology 16 :744–753.

Roff, D. A., and D. J. Fairbain. 2007. The evolution of trade-offs : where are we ? Journal of Evolutionary Biology 20 :433–447.

Roff, D. A., S. Mostowy, and D. J. Fairbairn. 2002. The evolution of trade-offs : testing predictions on response to selection and environmental variation. Evolution 56 :84–95.

Schmidt-Nielson, K. 1997. Movement, muscle, biomechanics. Animal physiology : adaptation and environment, 5th edition. Cambridge University Press, Cambridge, UK pages 395–463.

Sgrò, C. M., and A. A. Hoffmann. 2004. Genetic correlations, tradeoffs and environmental variation. Heredity 93 :241–248.

Stearns, S. C. 1989. Trade-offs in life-history evolution. Functional ecology 3 :259–268.

———. 1992. The evolution of life histories, vol. 249. Oxford University Press Oxford.

Tatar, M., A. Bartke, and A. Antebi. 2003. The endocrine regulation of aging by insulin-like signals. Science 299 :1346–1351.

Tucic, B., D. Pemac, and S. Avramov. 2005. Testing the predictions of an evolutionary trade-off model using iris pumila plants from an open and a shaded habitat. Plant species biology 20 :17–22.

Van Noordwijk, A. J., and G. de Jong. 1986. Acquisition and allocation of resources : their influence on variation in life history tactics. The American Naturalist 128 :137–142.

Verin, M., S. Bourg, F. Menu, and E. Rajon. 2017. The biased evolution of generation time. Am Nat 190 :E28–E39.

Wagner, A. 2005. Robustness and evolvability in living systems. Princeton University Press Princeton, NJ :.

Wagner, G. P., J. P. Kenney-Hunt, M. Pavlicev, J. R. Peck, D. Waxman, and J. M. Cheverud. 2008. Pleiotropic scaling of gene effects and the 'cost of complexity'. Nature 452 :470–472.

Wagner, G. P., and J. Zhang. 2011. The pleiotropic structure of the genotype–phenotype map : the evolvability of complex organisms. Nature Reviews Genetics 12 :204–213.

———. 2012. Universal pleiotropy is not a valid null hypothesis : reply to hill and zhang. Nature Reviews Genetics 13 :296–296.

Walker, R. S., M. Gurven, O. Burger, and M. J. Hamilton. 2008. The trade-off between number and size of offspring in humans and other primates. Proceedings of the Royal Society B : Biological Sciences 275 :827–834.

Williams, H., P. L. Johnson, L. Fenster, L. Laster, J. Field, et al. 1963. Intestinal glucose-6-phosphatase in control subjects and relatives of a patient with glycogen storage disease. Metabolism 12 :235–241.

Wright, S. 1931. Evolution in mendelian populations. Genetics 16 :97–159.

———. 1980. Genic and organismic selection. Evolution pages 825–843.

Zadik, Z., A. Chalew, R. J. McCarter JR, M. Meistas, and A. A. Kowarski. 1985. The influence of age on the 24-hour integrated concentration of growth hormone in normal individuals. The Journal of

Clinical Endocrinology & Metabolism 60 :513–516.

Zera, A. J., and L. G. Harshman. 2001. The physiology of life history trade-offs in animals. Annual review of Ecology and Systematics 32 :95–126.

Zera, A. J., and C. Zhang. 1995. Evolutionary endocrinology of juvenile hormone esterase in gryllus assimilis : direct and correlated responses to selection. Genetics 141 :1125–1134.

Zhao, Z., and A. J. Zera. 2002. Differential lipid biosynthesis underlies a tradeoff between reproduction and flight capability in a wing-polymorphic cricket. Proceedings of the National Academy of Sciences 99 :16829–16834.